Support Information

Three-dimensional $Ni_{0.85}Se$@ZnSe nanostrucures on carbon cloth for flexible asymmetric battery-type supercapacitor

Shuling Liu*, Rui Wang, Qiuting Wang, Xian Cui, Zeyu Liu

College of Chemistry & Chemical Engineering, Shaanxi University of Science & Technology,

Xi'an, Shaanxi 710021, PR China

Contents:

1. Electrochemical performance test

After washing, the electrode materials obtained by electrodeposition were put into a vacuum drying oven and dried for 12 h at 60 ℃. The electrolyte solution required for all electrochemical tests was 4 M KOH. The reference electrode, counter electrode and working electrode of the test system were Mercury oxide (Hg/HgO), platinum sheet electrode and electrodeposited active material electrode respectively. The voltage window range of cyclic voltammetry curve (CV) is set as 0-0.6V, and the voltage window range of constant current charge-discharge curve (GCD) is set as 0-0.5V (mono is: 0-0.45), the Energy Quest curve (EIS) was tested at an open circuit potential in the frequency range of 0.01Hz-100khz, and electrochemical performance was tested at the electrochemical workstation (CHI660E, Shanghai Chenhua). In the two-electrode test system, Ni0.85Se@ZnSe was used as the positive electrode and activated carbon (AC) as the negative electrode.

The discharge time (Δt) of the GCD curve is proportional to the electrochemical capacity (C_m, F g^{-1}) of the electrode material. Eq (S1) as follows:

$$C_m = \frac{I \times \Delta t}{m \times \Delta v} \tag{S1}$$

where I is the discharge current density (A g^{-1}); m represents the mass of active materials grown on CC for three-electrode configurations (g); Δt is the discharge time (s); and ΔV is the potential window (V).

The energy density (E, Wh kg^{-1}) and power density (P, W kg^{-1}) of the ASCs are were investigated by eqs (S2) and (S3), respectively, as follows:

$$E = \frac{C_m \times \Delta V^2}{3.6 \times 2} \tag{S2}$$

$$P = \frac{3600E}{\Delta t} \tag{S3}$$

2. Material characterization

The phase characterization of the sample $Ni_{0.85}Se$@ZnSe nanospheres was performed by X-Ray powder diffractometer (XRD, Japanese, Rigaku D/Max-3c) Cu Ka (λ=1.5418 Å), the test voltage was 40 kV; The morphology, energy spectrum (EDS) and elemental analysis (mapping) of the sample were characterized by emission scanning electron microscope (FE-SEM, Hitachi S-4800, Japan); X-ray electron spectroscopy (XPS, UK AXIS SUPRA (Kratos)) was used. The composition and valence state of the sample elements were analyzed; the transmission electron microscope (TEM, FEI Tecnai G2F20, USA) characterized the microstructure of the sample.

3. Supplementary figures

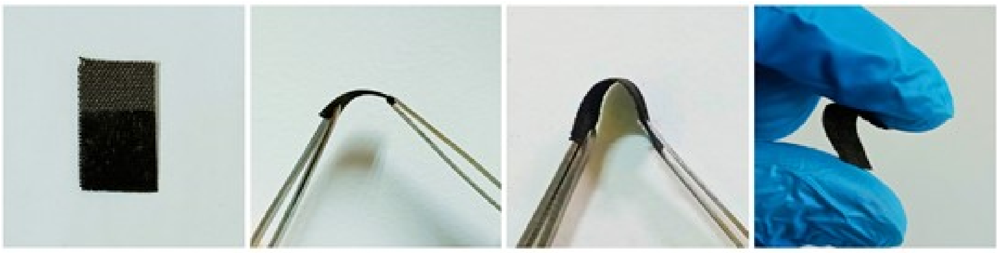

Figure S1. The photographs of the $Ni_{0.85}Se$@ZnSe CC electrode under folded and twisted conditions

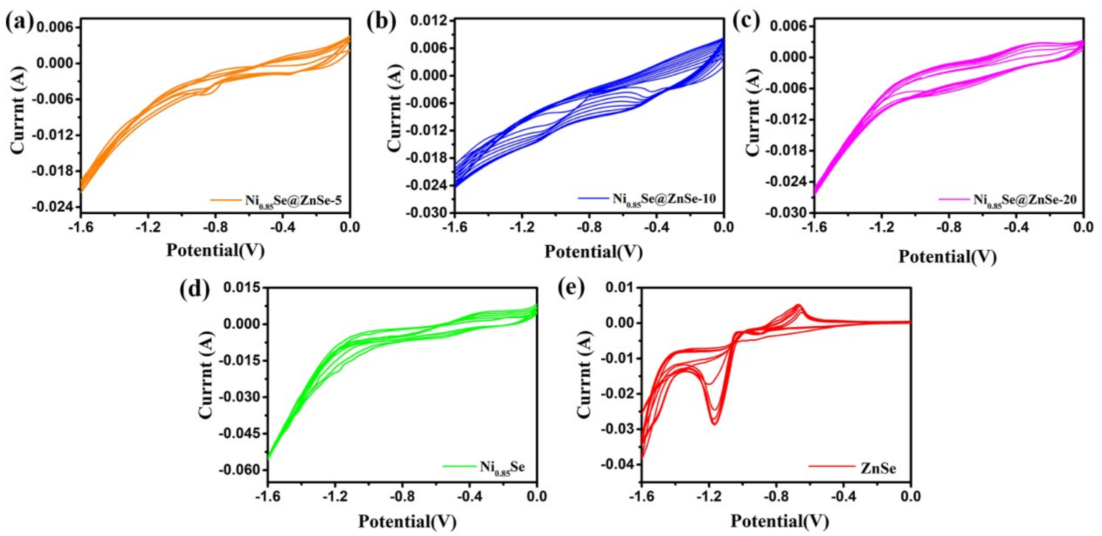

Figure S2. CV curves during electrodeposition process

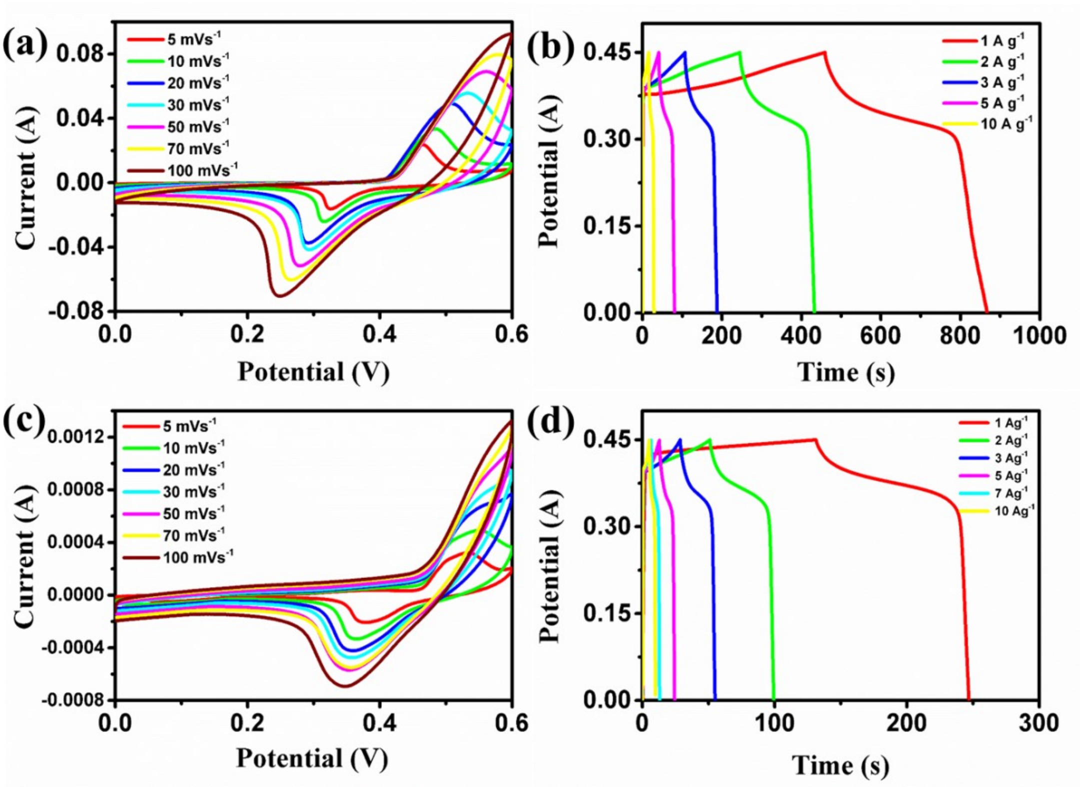

Figure S3. (a, c) CV curves of the $Ni_{0.85}Se$, ZnSe at different scan rates, (b, d) GCD curves of the $Ni_{0.85}Se$, ZnSe at different electric current density.

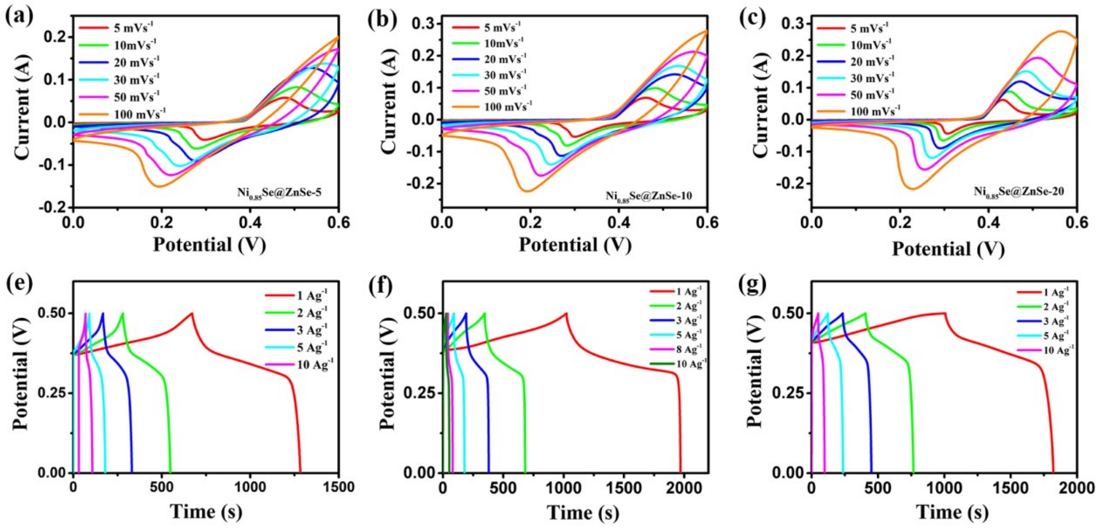

Figure S4. (a,b, c) CV curves of the $Ni_{0.85}Se$@ZnSe-5, $Ni_{0.85}Se$@ZnSe-10, $Ni_{0.85}Se$@ZnSe-20 at different scan rates, (d, e, f) GCD curves of the $Ni_{0.85}Se$@ZnSe-5, $Ni_{0.85}Se$@ZnSe-10, $Ni_{0.85}Se$@ZnSe-20 at different electric current density.

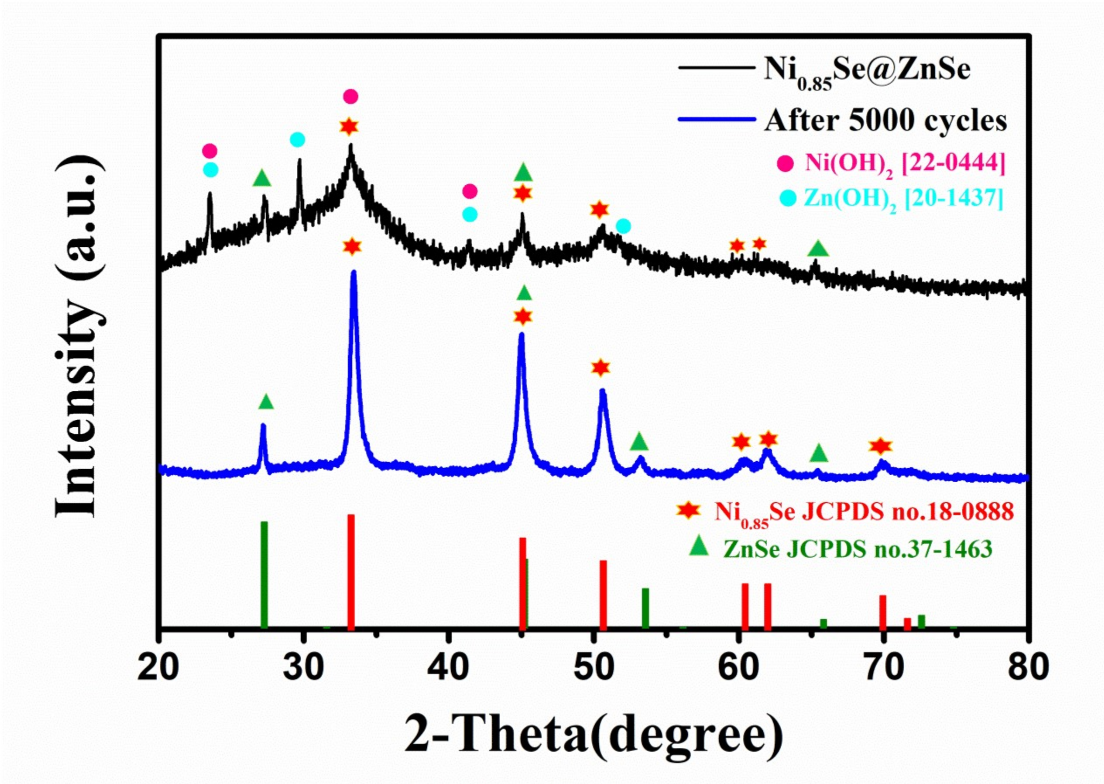

Figure S5. XRD patterns of the $Ni_{0.85}Se$@ZnSe-10 (blue line) and $Ni_{0.85}Se$@ZnSe-10 electrode after cycling tests (black line)

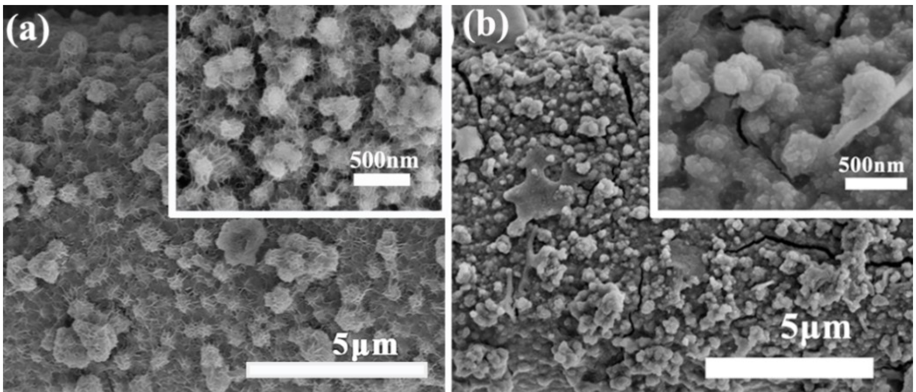

Figure S6. (a) SEM images of $Ni_{0.85}Se$@ZnSe-10, (b) SEM images of $Ni_{0.85}Se$@ZnSe-10 cycling at 10 A g^{-1} for 5000 times

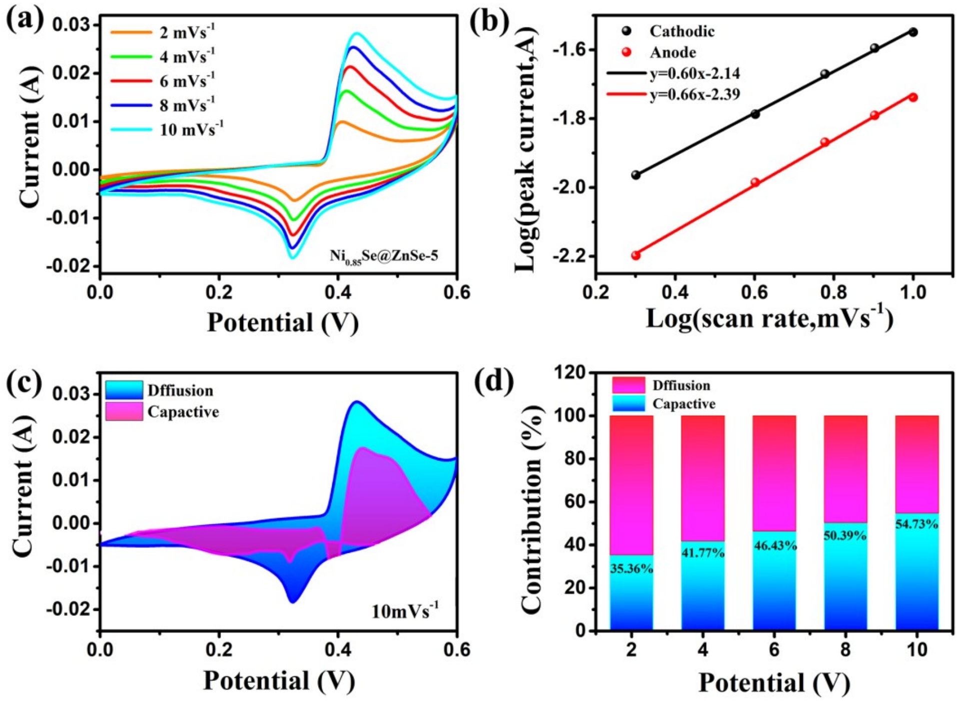

Figure S7. Quantitative capacitive analysis of energy storage behavior: (a) the CV curves of $Ni_{0.85}Se$@ZnSe-5, (b) the curves of log(i) and log(V), (c)the capacitive contribution for $Ni_{0.85}Se$@ZnSe-5 and diffusion contribution (blue) at a scan of 10 mV s^{-1}, (d) comparison of charge storage for $Ni_{0.85}Se$@ZnSe-5 electrodes at different scan rates.

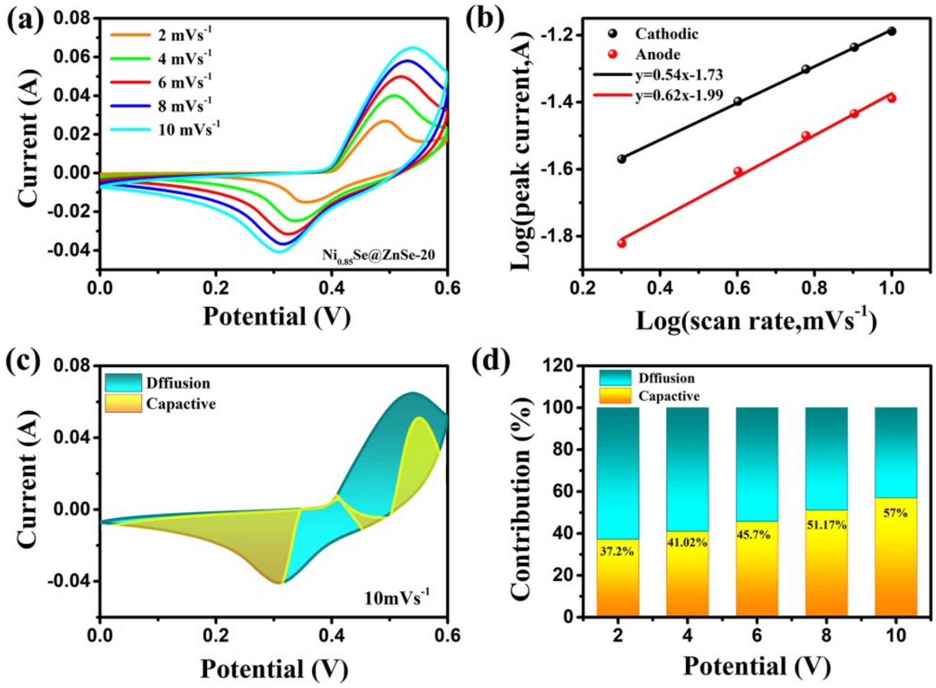

Figure S8. Quantitative capacitive analysis of energy storage behavior: (a) the CV curves of $Ni_{0.85}Se$@ZnSe-20, (b) the curves of log(i) and log(V), (c)the capacitive contribution for $Ni_{0.85}Se$@ZnSe-20 and diffusion contribution (blue) at a scan of 10 mV s^{-1}, (d) comparison of charge storage for $Ni_{0.85}Se$@ZnSe-20 electrodes at different scan rates.

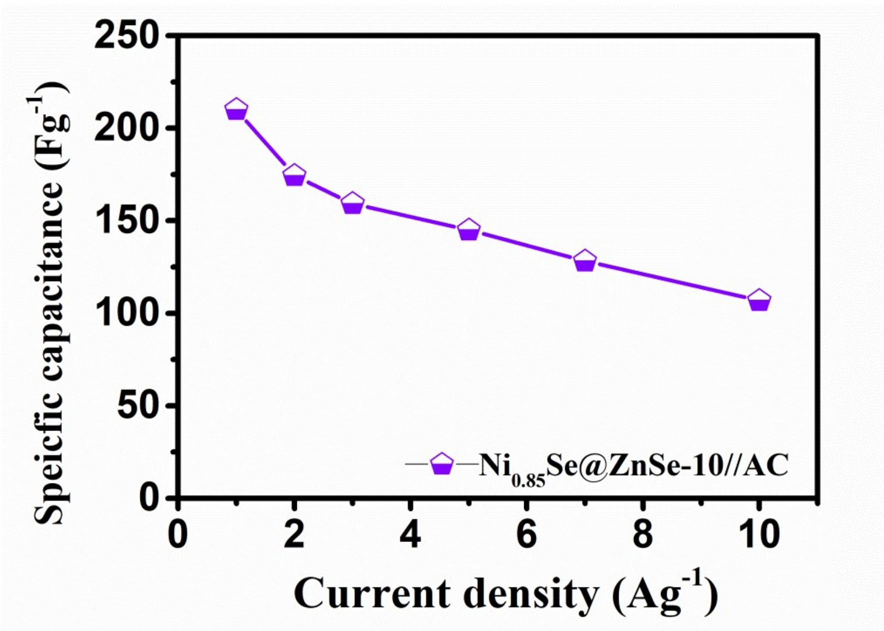

Figure S9. The capacity ratio of $Ni_{0.85}Se$@ZnSe-10//AC ACS

4. Supplementary tables S1-S4

Table S1. Fitted parameters of the Nyquist plots in Fig. 5f using equivalent circuits.

samples	R_s (Ω)	R_{ct} (Ω)
ZnSe	1.387	1.98
$Ni_{0.85}Se$	1.174	1.46
$Ni_{0.85}Se$@ZnSe-5	0.69	1.38
$Ni_{0.85}Se$@ZnSe-10	0.47	1.14
$Ni_{0.85}Se$@ZnSe-20	0.64	1.26

Table S2. The $Ni_{0.85}Se$@ZnSe-10 of elemental composition of Smart quant results by the EDS.

Element	***Wt%***	***At%***
SeL	58.14	52.83
NiK	24.06	29.45
ZnK	16.13	17.72

Table S3. The specific capacity (F g^{-1}) at different current densities in Figure 5e.

	1 A g^{-1}	**2 A g^{-1}**	**3 A g^{-1}**	**5 A g^{-1}**	**10 A g^{-1}**
ZnSe	258	216.5	187	138.9	118.5
$Ni_{0.85}Se$	917	832.5	538.7	467	405
$Ni_{0.85}Se$@ZnSe-5	1228	1077	992	900	766
$Ni_{0.85}Se$@ZnSe-10	1927	1629,	1448,	1310	1058
$Ni_{0.85}Se$@ZnSe-20	1674	1448	1296	1085	912

Table S4. Comparison of the capacity performance of as-prepared $Ni_{0.85}Se$@ZnSe and other metallic selenides electrode materials reported previously.

Electrode material	Special capacity	Morphology	Current density	Ref
$Ni_{0.85}Se$@ZnSe	nanostrucures	1927 F g^{-1}	1A g^{-1}	This work

$Ni_{0.85}Se@MoSe_2$	nanostructures	774 F g^{-1}	1 A g^{-1}	Manuscript 34
$NiFe_2Se_4$	particle-like microstructure	372.2 mA h g^{-1} (1339.92F g^{-1})	1 A g^{-1}	Manuscript 29
$NiCoSe_2$	nanostructure	2185 F g^{-1}	1 A g^{-1}	Manuscript 22
$NiMoO_4$	heterostructured	1061 F g^{-1}	2 A g^{-1}	Manuscript 36
$Cu_{0.5}Co_{0.5}Se_2$	nanosheets	1695 F g^{-1}	1 A g^{-1}	[1]
Mn-Co-Se	urchin-like	1656 F g^{-1}	1 A g^{-1}	[2]
$CoNi_2Se_4$	flake-like	1505 F g-1	1 A g^{-1}	[3]
$NiCoSe_2$	ellipsoid structure	1408 F g^{-1}	1 A g^{-1}	[4]
$Ni_{0.9}Co_{1.92}Se_4$	coral-like	510.55 C g^{-1} (1021.1 F g^{-1})	2 mA cm^{-2}	6
$(Ni,Co)Se_2$	cactus-like structure	972 F g^{-1}	2 A g^{-1}	7
Co-Cd-Se	nanorods	192 mA h g^{-1} (1382 F g^{-1})	1 A g^{-1}	[5]
$CoFe_2Se_4$-$CoNiSe_2$	composite	183.4 mA h g^{-1} (1320.5 F g^{-1})	1 A g^{-1}	8
$NiFe_2Se_4$	particle-like microstructure	126.9 F g^{-1}	1 A g^{-1}	9
Ni-Co-Se	hollow nanoparticles	584 C g^{-1} (1168 F g^{-1})	1 A g^{-1}	10
$Ni_{0.6}Co_{0.4}Se_2$	reed mat-like sheets	1580 F g^{-1}	1 A g^{-1}	11
$NiCo_2O_4$ @$Ni_{0.85}Se$	core-shell architecture	1454 F g^{-1}	1 A g^{-1}	13

Table S5 Comparison of the performance of $Ni_{0.85}Se@ZnSe$ //AC with those of reported HSC devices based on metallic selenides.

Supercapacitors	Specific energy (Wh Kg^{-1})	Specific power W Kg^{-1}	Ref
$Ni_{0.85}Se@ZnSe$ //AC ASC	74.67 Wh kg^{-1}	800 W kg^{-1}	This work
NFSe-20//AC	45.6 Wh kg^{-1}	800 W kg^{-1}	manuscript 29
$Ni_{0.85}Se@MoSe_2$//GNS	25.2 Wh kg^{-1}	420 W kg^{-1}	Manuscript 34
ZNSe@NCS@NF//AC@NF	52.37Wh kg^{-1}	800 W kg^{-1}	Manuscript 24
NCSe-5//AC	41.8Wh kg^{-1}	800W kg^{-1}	Manuscript 22
$NiMoO_4$//APC	31.8Wh kg^{-1}	786.5W kg^{-1}	Manuscript 36
$Cu_{0.5}Co_{0.5}Se_2$//Ti_3C_2	84.17 Wh kg^{-1}	604 W kg^{-1}	1
Mn-Co-Se//AC	55.1 Wh kg^{-1}	880 W kg^{-1}	2
$Ni_{0.9}Co_{1.92}Se_4$//AC	26.29 Wh kg^{-1}	265 W kg^{-1}	[6]
$(Ni,Co)Se_2$/NiCo-LDH//PC	39 Wh kg^{-1}	1650 W kg^{-1}	[7]
Co-Cd-Se// /Fe alkaline	57.6Wh Kg^{-1}	10.9 kW kg^{-1}	5
CFS–CNS//CFS–CN	80.2 W h kg^{-1}	1000 W kg-[1]	[8]
$NiFe_2Se_4$//AC	45.6 W h kg^{-1}	800 W kg^{-1}	[9]
Ni-Co-Se//RGO	41.8 W h kg^{-1}	750 W kg^{-1}	[10]
$Ni_{0.6}Co_{0.4}Se_2$//AC	44.1 W h kg^{-1}	691.3 W kg^{-1}	[11]
$(Ni,Cu)Se_2$ //AC	44.46 Wh kg^{-1}	797.9 W kg^{-1}	[12]
$NiCo_2O_4$ @$Ni_{0.85}Se$ //AC	29.3 Wh kg^{-1}	799 W kg^{-1}	[13]

6. Supplementary References

1. Dakka, Y. A.; Balamurugan, J.; Balaji, R.; Kim, N. H.; Lee, J. H. J. C. E. J., Advanced $Cu_{0.5}Co_{0.5}Se2$ nanosheets and MXene electrodes for high-performance asymmetric supercapacitors. *385 : 123455*.

2. Miao, C.; Xu, P.; Zhao, J.; Zhu, K.; Cheng, K.; Ye, K.; Yan, J.; Cao, D.; Wang, G.; Zhang, X., Binder-Free Hierarchical Urchin-like Manganese–Cobalt Selenide with High Electrochemical Energy Storage Performance. *ACS Applied Energy Materials* **2019,** *2* (5),

3595-3604.
3. Rajesh, J. A.; Lee, Y.-H.; Yun, Y.-H.; Vinh Quy, V. H.; Kang, S.-H.; Kim, H.; Ahn, K.-S., Bifunctional $NiCo_2Se4$ and $CoNi_2Se_4$ nanostructures: Efficient electrodes for battery-type supercapacitors and electrocatalysts for the oxygen evolution reaction. *Journal of Industrial and Engineering Chemistry* **2019,** *79*, 370-382.
4. Sakthivel, M.; Sukanya, R.; Chen, S. M.; Pandi, K.; Ho, K. C. J. R. e., Synthesis and characterization of bimetallic nickel-cobalt chalcogenides (NiCoSe_2, NiCo_2S_4, and NiCo_2O_4) for non-enzymatic hydrogen peroxide sensor and energy storage: Electrochemical properties dependence on the metal-to-chalcogen composition. **2019,** *138* (AUG.), 139-151.
5. Zhai, Z.-B.; Huang, K.-J.; Wu, X., Superior mixed Co-Cd selenide nanorods for high performance alkaline battery-supercapacitor hybrid energy storage. *Nano Energy* **2018,** *47*, 89-95.
6. An, W.; Liu, L.; Gao, Y.; Liu, Y.; Liu, J., $Ni_{0.9}Co_{1.92}Se_4$ nanostructures: binder-free electrode of coral-like bimetallic selenide for supercapacitors. *RSC Advances* **2016,** *6* (79), 75251-75257.
7. Li, X.; Wu, H.; Guan, C.; Elshahawy, A. M.; Dong, Y.; Pennycook, S. J.; Wang, J., (Ni,Co)Se2 /NiCo-LDH Core/Shell Structural Electrode with the Cactus-Like (Ni,Co)Se2 Core for Asymmetric Supercapacitors. *Small* **2019,** *15* (3), e1803895.
8. Gopi, C.; Reddy, A. E.; Kim, H. J. J. J. o. M. C. A., Wearable superhigh energy density supercapacitors using a hierarchical ternary metal selenide composite of CoNiSe2 microspheres decorated with CoFe2Se4 nanorods. **2018**, 10.1039.C8TA01141A.
9. Ye, B.; Cao, X.; Zhao, Q.; Wang, J., Electrodeposited $NiFe_2Se_4$ on Nickel Foam as a Binder-Free Electrode for High-Performance Asymmetric Supercapacitors. *Industrial & Engineering Chemistry Research* **2020,** *59* (31), 14163-14171.
10. Chen, H.; Fan, M.; Li, C.; Tian, G.; Lv, C.; Chen, D.; Shu, K.; Jiang, J. J. J. o. P. S., One-pot synthesis of hollow NiSe–CoSe nanoparticles with improved performance for hybrid supercapacitors. **2016,** *329*, 314-322.
11. Xie, S.; Gou, J.; Liu, B.; Liu, C. J. J. o. C.; Science, I., Nickel-cobalt selenide as high-performance and long-life electrode material for supercapacitor. **2019,** 540: 306-314**.**.
12. Bo, C.; Tian, Y.; Yang, Z.; Ruan, Y.; Jiang, J.; Wang, C. J. C., Construction of (Ni, Cu) Se2//Reduced Graphene Oxide for High Energy Density Asymmetric Supercapacitor. **2017,** *4* (11): 3004-3010.
13. Sui, Y.; Ye, A.; Qi, J.; Wei, F.; He, Y.; Meng, Q.; Ren, Y.; Sun, Z., Construction of $NiCo_2O_4$@$Ni_{0.85}Se$ core-shell nanorod arrays on Ni foam as advanced materials for an asymmetric supercapacitor. *Journal of Alloys and Compounds* **2019,** *778*, 234-238.